

Polymer Chemistry

Accepted Manuscript



This is an *Accepted Manuscript*, which has been through the Royal Society of Chemistry peer review process and has been accepted for publication.

Accepted Manuscripts are published online shortly after acceptance, before technical editing, formatting and proof reading. Using this free service, authors can make their results available to the community, in citable form, before we publish the edited article. We will replace this *Accepted Manuscript* with the edited and formatted *Advance Article* as soon as it is available.

You can find more information about *Accepted Manuscripts* in the [Information for Authors](#).

Please note that technical editing may introduce minor changes to the text and/or graphics, which may alter content. The journal's standard [Terms & Conditions](#) and the [Ethical guidelines](#) still apply. In no event shall the Royal Society of Chemistry be held responsible for any errors or omissions in this *Accepted Manuscript* or any consequences arising from the use of any information it contains.

Synthesis and Properties of a Rod-*g*-Rod Bottlebrush with a Semirigid Mesogen-Jacketed Polymer as the Side Chain

Hai-Jian Tian, Wei Qu, Yu-Feng Zhu, Zhihao Shen,* and Xing-He Fan*

Beijing National Laboratory for Molecular Sciences, Key Laboratory of Polymer Chemistry and Physics of Ministry of Education, College of Chemistry and Molecular Engineering, Peking University,
Beijing 100871, China

* To whom the correspondence should be addressed. E-mail: fanxh@pku.edu.cn;

zshen@pku.edu.cn.

Abstract: A series of bottlebrushes, Poly(γ -3-azidopropanyl-L-glutamate)-*g*-poly{2,5-bis[(4-methoxyphenyl)oxycarbonyl]styrene (PPLG-*g*-PMPCS), with an α -helical rigid backbone and mesogen-jacketed rigid side chains were synthesized by the “grafting onto” method from a yne-terminated PMPCS (side chain) and poly(γ -azide propanyl-L-glutamate) (backbone) by Cu(I)-catalyzed 1,3-dipolar cycloaddition click reaction. The chemical structures of the bottlebrushes were confirmed by ¹H NMR, gel permeation chromatography (GPC), GPC coupled with multi-angle laser light scattering and differential refractive index detectors, and Fourier-transform infrared spectroscopy. Bottlebrushes

were obtained with high grafting densities ($> 85\%$). Properties of the bottlebrushes were studied by small-angle X-ray scattering and atomic force microscopy. And the results show that the conformation of the bottlebrush changes from a cylinder to an ellipsoid as the degree of polymerization of the side chain increases from 14 to 65.

Introduction

Bottlebrushes are densely grafted polymers, with properties distinctly different from those of sparsely grafted or linear polymers.¹⁻⁴ Bulky side chains are packed around the backbone, and the steric effect between neighboring side chains forces the backbone to adopt a stretched conformation. Even with a flexible backbone and flexible side chains, a bottlebrush shows a rigid or worm-like conformation.^{5,6} When their structures are precisely tailored, bottlebrushes can be used to form nanowires^{7,8} and nanotubes.⁹⁻¹¹ Because of their complex structures, they were once difficult to synthesize. With the development of living and controlled polymerization and “click” strategy, now there are mainly three ways to synthesize a bottlebrush: “grafting onto”, “grafting through”, and “grafting from”.¹⁻⁴ With these methods, different bottlebrushes with flexible backbone, flexible side chains (coil-g-coil),^{5,6} with rigid backbone, flexible side chains (rod-g-coil),¹²⁻¹⁴ and with flexible backbone, rigid side chains (coil-g-rod)¹⁵ have been synthesized. However, bottlebrushes with rigid backbone, rigid side chains are rare¹⁶ because it is difficult to synthesize rigid chains by controlled and living polymerization. With a rigid backbone, the bottlebrush will be rigid even if the side chain is not so bulky; and with rigid side chains, the rigidity of the side chains will affect the main chain, making it stiffer.¹⁵ Therefore,

rod-g-rod bottlebrushes may have the advantage of forming ordered nanostructures with large dimensions, serving as potential candidates for nano-porous materials, photonic crystals, and so on.

Polypeptides are rigid polymers owing to their ability to form secondary structures (e.g., α -helix and β -sheet).¹⁷ In addition, they can be prepared by controlled ring-opening polymerization (ROP) of α -amino acid *N*-carboxyanhydrides (NCAs).^{18,19} These two factors make polypeptides attractive for building bottlebrushes. Bottlebrushes with polypeptides as backbones are synthesized by “grafting onto”^{12,20-23} and “grafting from” methods.^{13,24,25} In those studies, side-chain DP-dependent polymer properties, such as secondary structures²³ and thermo-responsive and self-assembling behaviors,²⁴ were studied. In addition to polypeptides, other rigid polymers like poly(*p*-phenylene terephthalamide)²⁶ or polyphenylene²⁷ can also be used as bottlebrush backbones. However, these polymers can not be obtained by controlled polymerization, which limits their studies.

On the other hand, mesogen-jacketed liquid crystalline polymers (MJLCPs) are also rigid polymers which have been extensively studied by our group.^{28,29} The origin of their rigidity is similar to that of bottlebrushes. Because in general bulky side groups (often mesogenic ones) are laterally attached directly to the backbone, the repulsion between neighboring side groups also forces the backbone to be extended.^{30,31} Dimensions of MJLCPs can be readily tuned by varying the mesogenic groups and molecular weights (MWs). Compared with other rigid polymers, MJLCPs can be easily prepared by controlled radical polymerizations. Therefore, they are excellent rod-like candidates for preparing rigid chains. A coil-g-rod bottlebrush with an MJLCP

as the side chain, polystyrene as the backbone (PS-*g*-PMPCS) has been previously reported by our group.³²

Herein, we report a rod-*g*-rod bottlebrush with poly(γ -azide propyl-L-glutamic acid) (PPLG) as the backbone, poly{2,5-bis[(4-methoxyphenyl)oxycarbonyl]styrene} (PMPCS) as the side chain. By combining atom transfer radical polymerization (ATRP), ROP of NCA, and Cu(I)-catalyzed click reaction, we successfully synthesized the bottlebrush PPLG-*g*-PMPCS with different side-chain lengths via the “grafting onto” strategy. Chemical structures of the bottlebrushes were characterized by ¹H NMR, Fourier-transform infrared spectroscopy (FT-IR), gel permeation chromatography (GPC), GPC coupled with multi-angle laser light scattering and differential refractive index detectors (GPC-MALLS-DRI), and the physical properties were examined by small-angle X-ray scattering (SAXS) and atomic force microscopy (AFM).

Experimental

Materials

2-Bromo-2-methylpropionyl bromide (98%, Acros), propargyl alcohol (99%, Aldrich), 1-chloro-3-hydroxypropane (98%, TCI), hexamethyldisilazane (HMDS, 98%, Acros), *N,N,N',N',N''*-pentamethyldiethylenetriamine (PMDETA, 98%, TCI), and triethylamine (98%, Acros) were used as received. *N,N*-Dimethylformamide (DMF), tetrahydrofuran (THF), and chlorobenzene were used after passing through activated columns under an argon atmosphere (M.Braun, Inc.). All other reagents were purchased from Beijing Chemical Reagents and used as received.

Methods

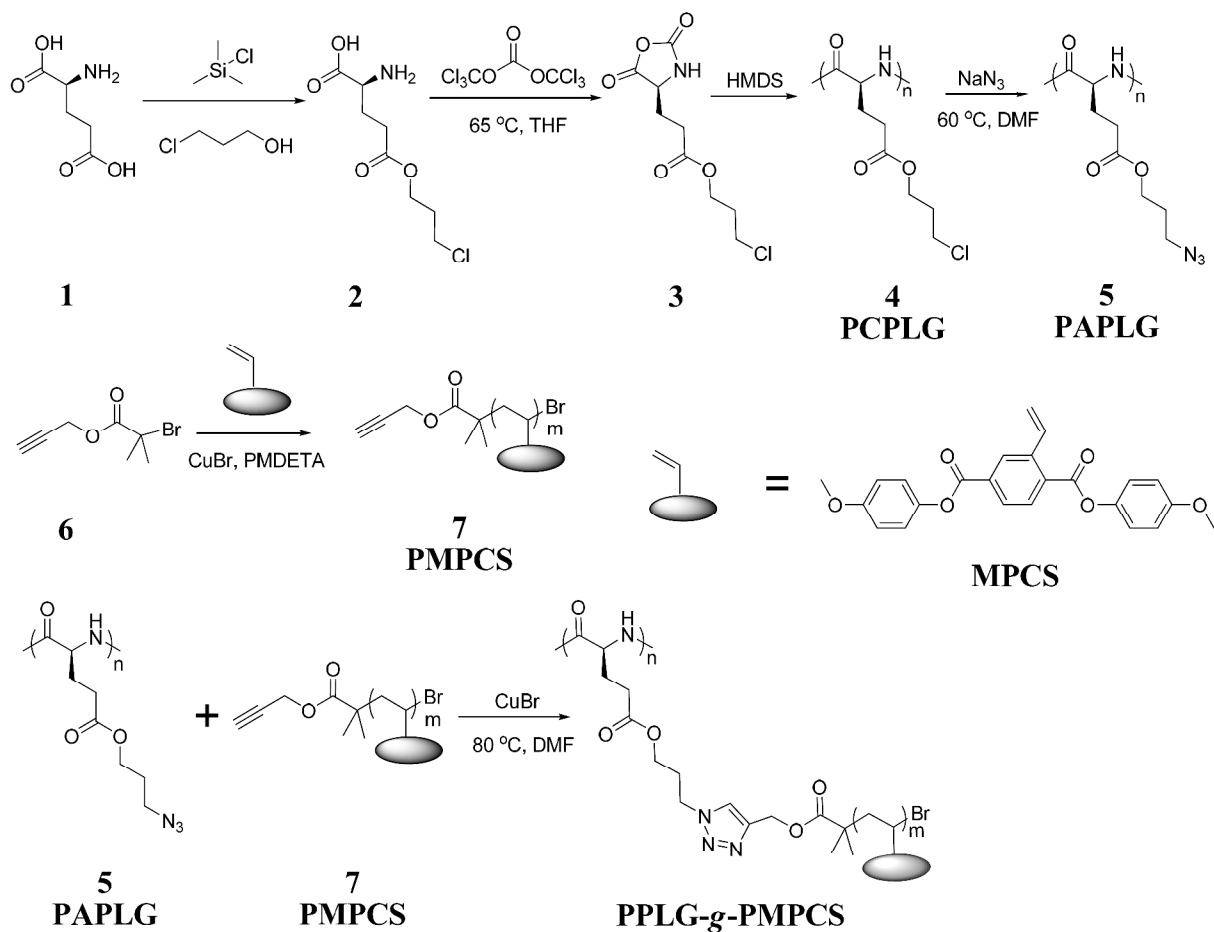
^1H NMR spectra were recorded on a Bruker AV-400 spectrometer. Matrix-assisted laser desorption/ionization-time of flight mass spectrometry (MALDI-TOF MS) measurements were performed on a Bruker Autoflex high-resolution tandem mass spectrometer. GPC experiments were conducted on a Waters 2410 instrument equipped with a Waters 2410 refractive index (RI) detector. THF with a flow rate of 1.0 mL/min was used as the eluent. Absolute MW of poly(γ -3-chloropropanyl-L-glutamate) (PCPLG) was determined by GPC-MALLS-DRI at 50 °C on an SSI pump connected to Wyatt Optilab DSP and Wyatt DAWN EOS light scattering detectors. DMF containing 0.02 M LiBr with a flow rate of 1.0 mL/min was used as the eluent. Absolute MWs of linear PMPCS and the bottlebrushes were determined by GPC-MALLS-DRI at 35 °C. THF with a flow rate of 1.0 mL/min was used as the eluent. Refractive index (RI) increments (dn/dc , using 1.0, 2.0, 3.0, 4.0, and 5.0 mg/mL) were measured off-line at ambient temperature at 658 nm using the Optilab Rex interferometric refractometer. For PCPLG in 0.02 M LiBr/DMF, $dn/dc = 0.0704$ mL/g (which was 0.0685 mL/g in 0.01 M LiBr/DMF²²). For the bottlebrush in THF, $dn/dc = 0.177$ mL/g, slightly larger than that of linear PMPCS ($dn/dc = 0.172$ mL/g³³). FT-IR was carried out using a Thermo Scientific Nicolet iN10-MX spectrophotometer between 4000 and 400 cm^{-1} at a spectral resolution of 4 cm^{-1} , and the number of scans was 16. SAXS measurements were performed on beamline BL16B1 using a three-slit system at Shanghai Synchrotron Radiation Facility. The wavelength of the X-ray was 0.124 nm. The two-dimensional (2D) SAXS patterns were recorded by a Mar165 CCD at a resolution of

2048×2048 pixels and a pixel size of 80 μm \times 80 μm for quantitative analysis. The sample-to-detector distance was 5248 mm for SAXS experiments (calibrated by beef tendon standard). AFM images were obtained at ambient conditions with a Multimode Nanoscope IIIa atomic force microscope (Veeco Metrology Group) in tapping mode. Polymers were transferred onto a PMPCS-modified silicon wafer³² by the Langmuir-Blodgett technology.

Synthesis of the bottlebrushes

The PPLG-*g*-PMPCS bottlebrushes were successfully synthesized by combining ATRP, ROP of NCA, and Cu(I)-catalyzed click reaction (Scheme 1) through the “grafting onto” strategy. The detailed synthetic routes are described as follows.

Scheme 1. Synthetic Pathways of the Backbone, Side chains, and the Bottlebrushes



Synthesis of azide-substituted poly(L-glutamate) (PAPLG, 5)

Azide-substituted poly(L-glutamate) was synthesized from γ -chloropropyl-L-glutamate by the method described in literature.²² Their synthetic method and the polymer properties are described in Supporting Information.

Synthesis of α -alkyne PMPCS (7)

PMPCS is a typical MJLCP, which has been systematically studied by our group.^{34,35} With an alkynyl-substituted ATRP initiator (**6**), an α -alkyne PMPCS was easily obtained.^{32,36} The synthetic method and the polymer properties are described in Supporting Information.

Synthesis of poly(γ -3-azidopropanyl-L-glutamate)-*g*-poly{2,5-bis[(4-methoxyphenyl)oxycarbonyl]styrene} (PPLG-*g*-PMPCS) by click reaction

A typical click procedure is described as follows. α -Yne-terminated PMPCS (7, 500 mg, $M_n = 9.8 \times 10^3$ g/mol, 51 μ mol yne groups), PPLG (5, 7.2 mg, 34 μ mol azide groups), and CuBr (4.8 mg, 34 μ mol) were introduced into a Schlenk flask and dissolved in DMF (30 mL). The Schlenk flask was degassed by three freeze-pump-thaw cycles, sealed under vacuum, and then immersed into an oil bath thermostated at 80 °C for 2 days. The solution was then cooled to ambient temperature and passed through a neutral alumina column to remove Cu(I) catalyst. The raw product was precipitated in methanol.

Reprecipitation

In a general procedure, 500 mg of the raw bottlebrush was dissolved in 20 mL of CH₂Cl₂. An equal volume of acetone was added to the solution. Methanol (20 mL) was added dropwise to the solution until it was turbid. The suspension was collected by centrifugation. This procedure was repeated twice to remove the unreacted PMPCS (52% yield).

Results and Discussion

Synthesis of the bottlebrushes via the “grafting onto” strategy

There are mainly three ways to synthesize a bottlebrush: “grafting onto”, “grafting through”, and “grafting from”. Compared to the other two strategies, the “grafting onto” strategy has the

advantages over control of backbone length, side-chain length, and polydispersity. The only problem is the control of the grafting density. Following the development of click reaction, this strategy leading to high grafting densities becomes popular.

The backbone (PAPLG) and side chains (PMPCS) were synthesized separately. Azide and yne groups are needed in Cu(I)-catalyzed 1,3-dipolar cycloaddition click reaction. Compared with yne-ended γ -propargyl-L-glutamate which is a liquid,¹² γ -chloropropanyl-L-glutamate (**2**) is a solid at ambient temperature, which makes purification and the next step (ROP of NCA) easier. HMDS was used as the initiator in the controlled ROP of the *N*-carboxyanhydride based on γ -3-chloropropanyl-L-glutamic acid (CPLG-NCA). PCPLG with an absolute MW of 25.9×10^3 g/mol and a low polydispersity index (PDI) of 1.04 was obtained (Figure S3 in Supporting Information). Treated with NaN_3 in DMF at 60 °C for two days, PCPLG was converted to PAPLG. ^1H NMR result demonstrates a quantitative conversion (Figure S4 in Supporting Information, peak a). The FT-IR spectrum of PAPLG (Figure S5 in Supporting Information, $\nu_{\text{N}=\text{N}=\text{N}} = 2095 \text{ cm}^{-1}$) reveals the presence of the azide group.

α -Alkyne PMPCS was synthesized by ATRP. With precise control of the feeding ratio, time, and temperature, a series of α -alkyne PMPCS samples with different MWs were synthesized. GPC traces are shown in Figure 1. Table 1 summarizes the polymerization results. As in our previous work,³⁶ the absolute MW of linear PMPCS is approximately 1.52 times of the value of number-average MW (M_n) from GPC. In this study, when the MW is relatively small, this relationship is true (entries 1~3). However, as the MW becomes larger, this relationship may not hold (entries 4 and 5). Therefore, we chose GPC-MALLS to determine the absolute MWs.

Table 1. Polymerization Results and MW Characteristics of α -Alkyne PMPCS Samples

Entry	$[M]_0/[I]_0$	Temperature (°C)	Time (h)	M_n (10^3 g/mol) ^a	PDI ^a	M_w (10^3 g/mol) ^b	DP
1	20	80	2	3.8	1.05	5.7	14
2	30	80	6	6.5	1.07	9.8	24
3	50	80	6	9.2	1.10	14.1	36
4	75	90	12	13.2	1.09	21.9	55
5	90	100	12	15.0	1.10	26.3	64

^a Determined by GPC (calibrated with polystyrene standards).

^b Determined by GPC-MALLS (THF) with $dn/dc = 0.172$, revised according to the results from MALDI-TOF.

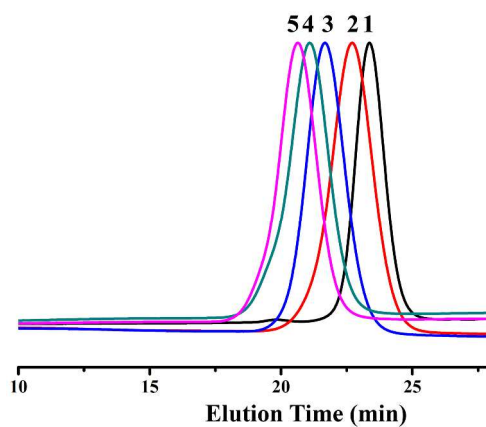


Figure 1. GPC traces of α -alkyne PMPCS: PMPCS₁₄ (1), PMPCS₂₄ (2), PMPCS₃₆ (3), PMPCS₅₅

(4), and PMPCS₆₄ (5).

In the synthesis of bottlebrushes, the same PCPLG backbone (absolute $M_w = 25.9 \times 10^3$ g/mol, PDI = 1.04) was used. α -Alkyne PMPCS was attached to the backbone by copper-catalyzed alkyne-azide [2+3] 1,3-dipolar cycloaddition. In order to obtain a high grafting density, the ratio of alkyne to azide groups was set to 1.5:1. Bottlebrushes were more difficult to dissolve in acetone compared to linear PMPCS, which made purification easier. The successful synthesis of the bottlebrushes was verified by GPC (Figure 2). ¹H NMR result shows that the signal of the alkyne group disappears after click reaction (Figure S6 in Supporting Information). The molecular weights were measured by GPC-MALLS (Table 2).

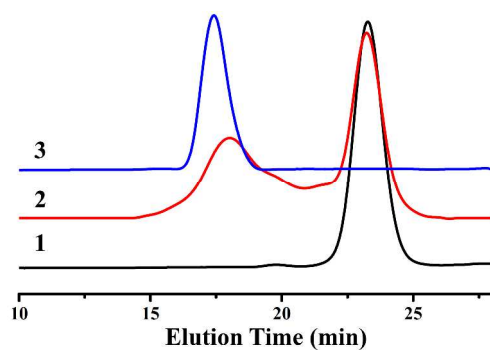


Figure 2. Representative GPC traces of PMPCS₁₄ (1), the blend after click reaction (2), the bottlebrush PPLG₁₂₆-g-PMPCS₁₄ (3). Because PAPLG forms aggregates in THF, the GPC curve of PAPLG is not shown.

Table 2. Compositional Parameters of PPLG-g-PMPCS Bottlebrushes

Bottlebrush ^a	$M_{w,side\ chain}$	PDI ^c	DP _{side chain}	$M_{w,bottlebrush}$	PDI ^d	Y_{graft}
--------------------------	---------------------	------------------	--------------------------	---------------------	------------------	-------------

	$(10^3 \text{ g/mol})^b$			$(10^6 \text{ g/mol})^d$		$(\%)^e$
PPLG ₁₂₆ -g-PMPCS ₁₄	5.7	1.05	14	0.67	1.06	90
PPLG ₁₂₆ -g-PMPCS ₂₄	9.8	1.07	24	1.20	1.02	95
PPLG ₁₂₆ -g-PMPCS ₃₆	14.1	1.10	36	1.60	1.01	87
PPLG ₁₂₆ -g-PMPCS ₅₅	21.9	1.09	55	2.49	1.03	88
PPLG ₁₂₆ -g-PMPCS ₆₄	26.3	1.10	64	2.99	1.03	90

^a Synthesized with PPLG₁₂₆ and PMPCS of different lengths.

^b Determined by GPC-MALLS (THF) with $dn/dc = 0.172$, revised according to results from MALDI-TOF MS.

^c Determined by GPC (calibrated with polystyrene standards).

^d Determined by GPC-MALLS (THF) with $dn/dc = 0.177$.

^e Grafting density $Y_{\text{graft}} = [(M_{w,\text{bottlebrush}} - M_{w,\text{backbone}}) / M_{w,\text{side chain}}] / DP_{\text{backbone}}$.

In our previous work,³² bottlebrushes with a polystyrene backbone shows a downward trend of grafting density (from 92% to 75%) as the MW of the backbone is increased, probably because the azide groups are embedded in the coil PS chains and it is difficult for them to be accessed for click reaction when the grafting density is increased. As for a helical polypeptide, the azide groups outside the helix are more accessible for yne-encapped side chains to react. In this work, the grafting density is in the range of 88~95%.

Because the content of the backbone is quite low in the bottlebrush, traditional characterization methods such as ^1H NMR (Figure S6 in Supporting Information) and FT-IR (Figure S7 in Supporting Information) show little or no difference between the side-chain polymers and bottlebrushes, which makes the characterization challenging.

Structural studies by SAXS

Scattering studies, including laser light scattering,^{15,37,38} SAXS,^{15,38,39} and small-angle neutron scattering (SANS),^{37,40-42} and AFM^{23,43} are usually used to study the nanostructures of bottlebrushes. In order to study the sizes and shapes of the bottlebrushes, SAXS measurements were carried out on solutions of the bottlebrushes in THF at a concentration of 1 mg/mL at 25 °C. As shown in Figure 3, SAXS analysis was performed over a q (scattering vector) range of 0.08 to approximately 0.8 nm^{-1} , which provides information on the overall size ($q = 0.08\text{--}0.2 \text{ nm}^{-1}$) as well as the cross-sectional size and particle shape ($q = 0.2\text{--}0.8 \text{ nm}^{-1}$).

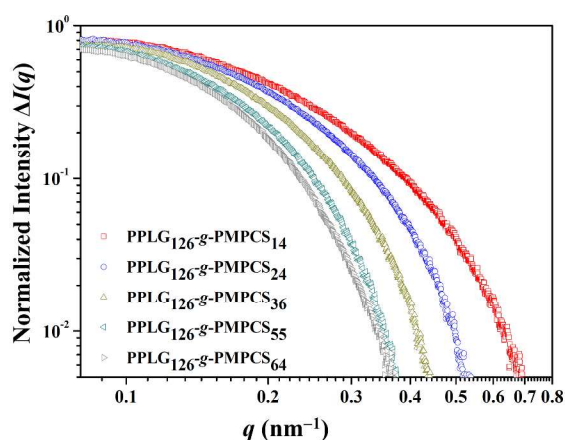


Figure 3. Double-logarithmic plots of the SAXS profiles of the bottlebrushes with side chains of different DPs.

We first utilized model-independent methods to analyze the SAXS data. According to Guinier,⁴⁴ the size parameter, radius of gyration (R_g), can be extracted directly from the Guinier plot (Figure S8 in Supporting Information) at small q values following equation (1):

$$\ln[\Delta I(q)] = \ln[a_0] - \frac{1}{3} R_g^2 q^2 \quad (1)$$

And for bottlebrushes, which are cylindrical particles, the cross-sectional radius of gyration ($R_{g,c}$) can also be determined by equation (2):⁴⁵

$$\ln[q\Delta I(q)] = \ln[b_0] - \frac{1}{2} R_{g,c}^2 q^2 \quad (2)$$

Here, $\Delta I(q)$ is the experimental excess scattering intensity. Data are calculated using primus in the ATSAS software package.⁴⁶ The results are summarized in Table 3.

Table 3. Parameters of the Bottlebrushes Obtained from Guinier Plots

Bottlebrush	R_g (nm)	$R_{g,c}$ (nm)	R_c (nm)^a
PPLG ₁₂₆ -g-PMPCS ₁₄	7.96	3.73	5.27
PPLG ₁₂₆ -g-PMPCS ₂₄	8.56	4.71	6.66
PPLG ₁₂₆ -g-PMPCS ₃₆	9.49	5.98	8.46
PPLG ₁₂₆ -g-PMPCS ₅₅	10.60	7.60	10.75
PPLG ₁₂₆ -g-PMPCS ₆₄	11.20	7.94	11.23

^a R_c is cross-sectional radius of the bottlebrush. For a circular homogeneous cylinder,

$$R_c = \sqrt{2}R_{g,c}$$

Guinier plots can give information about the overall or cross-sectional size. As the side-chain DP increases, R_g and $R_{g,c}$ increase. However, from the Guinier plots, little or no information about the particle structure can be obtained. Another model-independent analysis, indirect Fourier transform (IFT), gives the pair-distance-distribution functions (PDDFs, $p(r)$'s). PDDF profiles give indications about the particle shape: spherical, prolate, or oblate. In addition, radius of gyration, R_g , can also be given by the following equation (3):

$$R_{g,IFT} = \frac{1}{2} \frac{\int_0^{D_{max}} p(r) r^2 dr}{\int_0^{D_{max}} p(r) dr} \quad (3)$$

PDDFs are calculated using GNOM in the ATASA software package⁴⁷ (Figure 4 and Table S1 in Supporting Information). The obtained asymmetrical PDDF plots indicate elongated shapes. With increasing side-chain DP, the largest dimension increases slightly (Table S1 in Supporting Information), and the asymmetry of the plot decreases, which means that the particle becomes less elongated. $R_{g,IFT}$ values calculated from PDDFs are also presented in Table S1 in Supporting Information. $R_{g,IFT}$ increases as the side-chain DP increases.

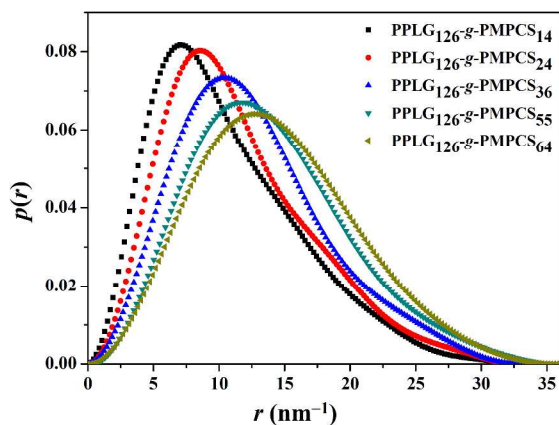


Figure 4. Calculated PDDFs for the bottlebrushes with side chains of different DPs.

To further study the shapes of the bottlebrushes, model-dependent methods are used to analyze the form factors. Three different models, cylinder, ellipsoid, and wormlike chain (WLC) models, are used to fit the SAXS profiles and obtain the form factors. The fittings were done by SASfit software package.^{40,42} From the fitting results, particle sizes, shapes, and chain stiffness can be estimated (See details in Supporting Information). The results are comparable with those from the Guinier plots and the PDDFs.

Figure 5 shows the R_g values obtained from different methods. There is no distinct difference between these methods. As the side-chain DP increases, the size of the bottlebrush increases. The cross-sectional radius R_c is associated with the length of the side chain. With increasing side-chain DP, N_s , a power-law dependence, $R_c \approx N_s^\xi$, is found (Figure 6), where $\xi = 0.44\text{--}0.52$ for different methods. The value of ξ is consistent with those in literature,^{37,41} which suggests a three-dimensional self-avoiding walk conformation of the bottlebrush side chain.⁴⁸

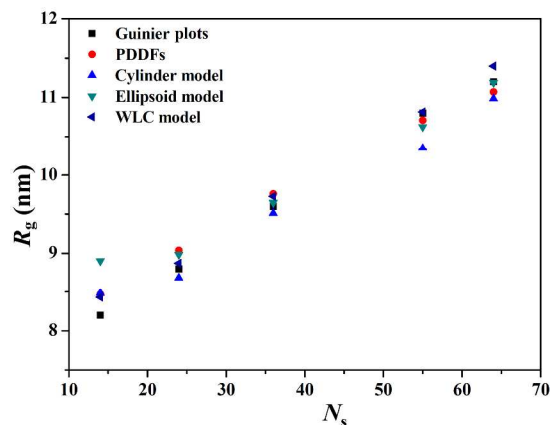


Figure 5. R_g values calculated from various methods for the bottlebrushes with side chains of different DPs.

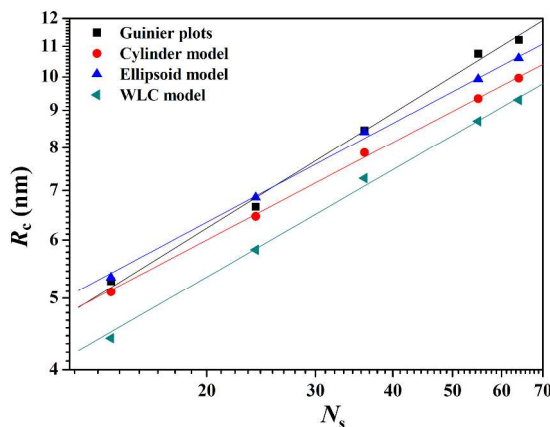


Figure 6. R_c values calculated from various methods for the bottlebrushes with side chains of different DPs, with the solid line representing a power-law fit to the data.

Compared with those from bottlebrushes having flexible PS side chains⁴¹ (Figure 7), R_c values of bottlebrushes with MJLCP side chains are almost two times larger at the same side-chain DP. For short side chains, the linkage between side chains and the backbone may play a large role. However, when the side-chain DP is large enough ($N_s > 50$), the linkage can be

ignored (a 9-atom spacer for PNB-g-PS, and 14-atom for PPLG-g-PMPCS). This dramatic difference in the cross-sectional radius is caused by the rigid structure of PMPCS, which has an extended-chain conformation because of the bulky mesogenic group.

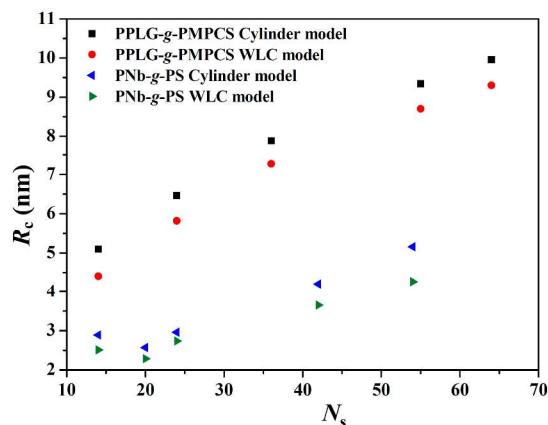


Figure 7. R_c values from the cylinder model and the WLC model for the bottlebrushes with side chains of different DPs. Data are compared with those from bottlebrushes having flexible side chains, PNB-g-PS, from literature.⁴¹

From the cylinder model, we can evaluate the particle length, which can be used to estimate the length of the backbone.³⁷ As the side-chain DP increases, the length of the cylinder (L_{cyl}) increases slightly (Figure 8). Such an increase may be caused by the side chains near the ends or the increased steric effect caused by neighboring side chains of larger DPs. The average length of the cylinder is $L_m = 27.1$ nm. Because the number-average DP for the polypeptide backbone is $N_m = 126$, the average length per monomeric unit $l_m = L_m/N_m = 27.1/126$ nm = 0.215 nm. For polypeptide, this value suggests a stretched helical conformation.²³

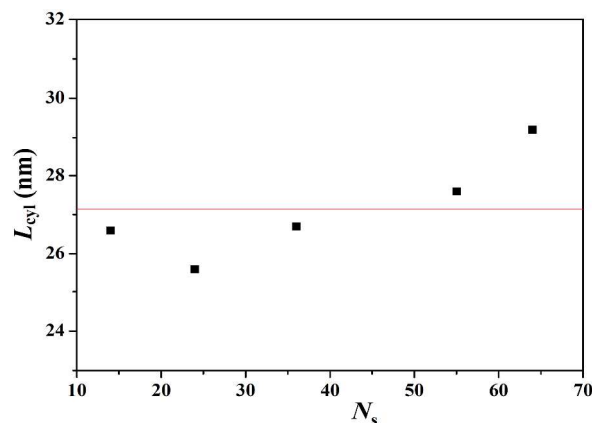


Figure 8. Length of the cylinder, L_{cyl} , according to the cylinder model for the bottlebrushes with side chains of different DPs.

The ellipsoid model gives the information about the cross-sectional radius R_c and the ratio between the two ellipsoidal axes (ν). As the side-chain DP increases, R_c increases, and ν decreases (Figure 9). We also calculated the asphericity parameter (α_s), which is used to quantify the deviation from the spherical shape (α_s can be any value between 0 and 1, with 0 representing a perfect sphere and 1 representing an infinitely long rod).⁴⁹ In this work, $0.2 < \alpha_s < 0.7$, indicating that the bottlebrushes are not perfect spheres, nor are they perfect long cylinders. As the side-chain DP increases, α_s decreases, which means that the particle looks more like a sphere, in other words, less elongated. This is consistent with the conclusion from the PDDF results and in good agreement with the work by Cheng and coworkers.⁴⁰ They used SANS to study the structure of polystyrene grafted with oligo(ethylene glycol). When the DP of the backbone increases, polymer conformation changes from an ellipsoid to a rigid cylinder, then to a wormlike chain. In this work, with increasing side-chain DP, conformational change of nanorods

is opposite. A similar result is also reported recently by Pesek and coworkers.⁴¹

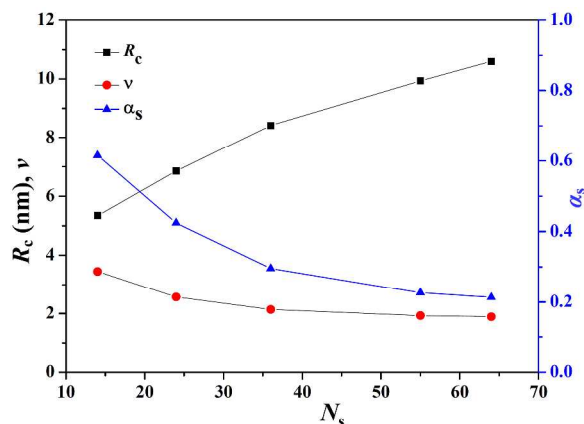


Figure 9. Cross-sectional radius (R_c), the ratio between the two ellipsoidal axes (v), and asphericity parameter (α_s) of particles for the bottlebrushes with side chains of different DPs according to the ellipsoid model.

As the side-chain DP increases, the stiffness characterized by the persistence length (l_p) of the backbone increases (Figure 10). The l_p values studied here are rather small compared with results in literature,^{37,48} smaller than that of poly(γ -benzyl- α -L-glutamate),⁵⁰ which has the same backbone as the bottlebrushes in this work. However, there are also several works reporting small l_p values of bottlebrushes in literature.^{41,42} Here, the bottlebrushes were synthesized from the “grafting onto” method, and the grafting density can not reach 100%. Therefore, the steric effect caused by neighboring side chains may not be large enough. And the linkage between side chains and the backbone may also relieve the steric constraint.⁴¹ In addition, the bottlebrushes studied here have a backbone of a modest length ($L_c = 45$ nm) with a rather long contour length ($R_c = 5$ – 10 nm). Thus, whether the WLC model is suitable here is still doubtful.

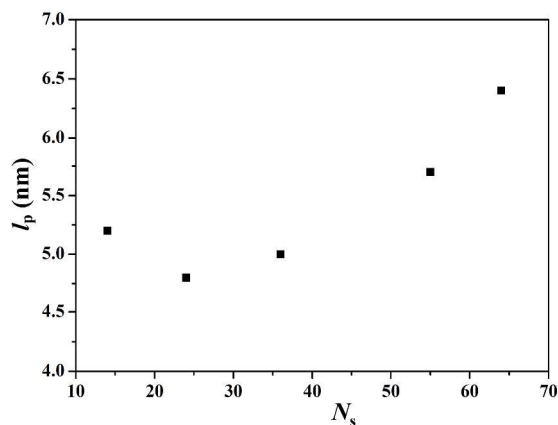


Figure 10. Values of persistence length, l_p , according to the wormlike chain model for the bottlebrushes with side chains of different DPs.

Morphological studies by AFM

Besides SAXS, AFM is also frequently used to study bottlebrushes, especially for imaging.⁴³ AFM was also used to image the rod-g-rod bottlebrushes. PMPCS-grafted bottlebrushes prefer to aggregate on unmodified silicon wafer.³² In order to obtain a unimolecular image, all the silicon wafers used were grafted with PMPCS homopolymers. Sample images (Figure 11) show a monolayer film on silicon wafers obtained by the Langmuir-Blodgett technology. Uniform nanoscaled rods with a length of about 25 nm are packed densely on the surface. As the backbone length is fixed, the nanorods show a similar length. From the AFM images, we can obtain the length of the cylinder, shown in Table 4. The average length per monomeric unit (l_m) can be calculated, and $l_m = 0.23\text{--}0.24$ nm, consistent with values in literature.²³ However, l_m is larger than that in solution. For PPLG₁₂₆-g-PMPCS₂₄, the cross-sectional radius from the cylinder model is 6.46 nm in the THF solution. When the bottlebrush is adsorbed on the silicon wafer, the

height is almost 2.5 nm (Figure 11f), much smaller than $2R_c$ (12.9 nm), which means that the side chains are flattened on the surface. This adds to the steric effect and makes the backbone more stretched, and the average length per monomeric unit becomes larger. Furthermore, the structure of the bottlebrush changes from a thin rod to a round ellipsoid as the side-chain DP increases (from Figure 11a to Figure 11e).

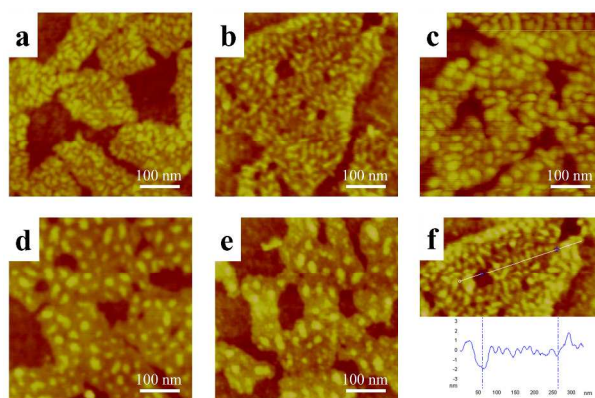


Figure 11. AFM images of the bottlebrushes with side chains of different DPs: PPLG₁₂₆-g-PMPCS₁₄ (a), PPLG₁₂₆-g-PMPCS₂₄ (b), PPLG₁₂₆-g-PMPCS₃₆ (c), PPLG₁₂₆-g-PMPCS₅₅ (d), PPLG₁₂₆-g-PMPCS₆₄ (e), and height profile of PPLG₁₂₆-g-PMPCS₂₄ (f).

Table 4. Sizes of the Bottlebrushes Obtained from AFM Results

Bottlebrush	h (nm) ^a	E (nm) ^b	L_s (nm) ^c	l_s (nm) ^d	L_m (nm) ^e	l_m (nm) ^f
PPLG ₁₂₆ -g-PMPCS ₁₄	2.1	5.4	—	—	—	—
PPLG ₁₂₆ -g-PMPCS ₂₄	2.4	5.7	10	0.21	29	0.23
PPLG ₁₂₆ -g-PMPCS ₃₆	2.5	5.8	15	0.21	29	0.23
PPLG ₁₂₆ -g-PMPCS ₅₅	2.6	5.9	24	0.22	30	0.24

PPLG ₁₂₆ -g-PMPCS ₆₄	3.0	6.2	28	0.22	30	0.24
--	-----	-----	----	------	----	------

^a Heights of the bottlebrushes.

^b Errors caused by the tip size, determined from $E = \sqrt{H(2R_c - H)}$,⁵¹ where R_c is the tip radius, $R_c = 8$ nm, and H is the height of the sample.

^c Length of the side chains, calculated using $L_s = L - 2E$, L is the value directly measured from the AFM images.

^d $l_s = L/N_s$.

^e Lengths of the bottlebrushes.

^f $l_m = L/N_m$, $N_m = 126$.

Conclusions

In summary, a series of bottlebrushes containing a rod backbone and rod side chains, PPLG-g-PMPCS, with different side-chain DPs were successfully synthesized by the combination of ATRP, ROP, and click reaction. Structures of the bottlebrushes were studied by SAXS and AFM. The results demonstrate a transformation from a rod to an ellipsoid as the side-chain DP increases. Although the stiffness of this kind of bottlebrushes is not as high as one would expect because the grafting density is not 100% and there is a flexible linkage between the side chains and the backbone, these bottlebrushes with rigid PMPCS side chains have longer side-chain lengths compared to those having flexible polystyrene side chains with the same side-chain DP, which may be used to build nano-porous materials with large pore sizes.

Supporting Information. The details for the synthesis of the PPLG-g-PMPCS bottlebrushes, ^1H NMR results, GPC curves, FT-IR spectra, fitting to the SAXS curves, and derived parameters.

Acknowledgment. This research was supported by the National Natural Science Foundation of China (Grants 21134001 and 20990232). The authors also thank the Shanghai Synchrotron Radiation Facility for assistance during SAXS experiments.

References and Notes

- (1) Zhang, M. F.; Muller, A. H. E. *J. Polym. Sci., Part A: Polym. Chem.* **2005**, *43*, 3461-3481.
- (2) Sheiko, S. S.; Sumerlin, B. S.; Matyjaszewski, K. *Prog. Polym. Sci.* **2008**, *33*, 759-785.
- (3) Potemkin, I. I.; Palyulin, V. V. *Polym. Sci. Ser. A* **2009**, *51*, 123-149.
- (4) Feng, C.; Li, Y.; Yang, D.; Hu, J.; Zhang, X.; Huang, X. *Chem. Soc. Rev.* **2011**, *40*, 1282-1295.
- (5) Terao, K.; Takeo, Y.; Tazaki, M.; Nakamura, Y.; Norisuye, T. *Polym. J.* **1999**, *31*, 193-198.
- (6) Terao, K.; Nakamura, Y.; Norisuye, T. *Macromolecules* **1999**, *32*, 711-716.
- (7) Zhang, M. F.; Estournes, C.; Bietsch, W.; Muller, A. H. E. *Adv. Funct. Mater.* **2004**, *14*, 871-882.
- (8) Yuan, J. Y.; Xu, Y. Y.; Walther, A.; Bolisetty, S.; Schumacher, M.; Schmalz, H.; Ballauff, M.; Muller, A. H. E. *Nat. Mater.* **2008**, *7*, 718-722.
- (9) Huang, K.; Rzyayev, J. *J. Am. Chem. Soc.* **2009**, *131*, 6880-6885.
- (10) Huang, K.; Canterbury, D. P.; Rzyayev, J. *Macromolecules* **2010**, *43*, 6632-6638.
- (11) Huang, K.; Rzyayev, J. *J. Am. Chem. Soc.* **2011**, *133*, 16726-16729.
- (12) Engler, A. C.; Lee, H.-i.; Hammond, P. T. *Angew. Chem.-Int. Edit.* **2009**, *48*, 9334-9338.

- (13) Liu, Y.; Chen, P.; Li, Z. B. *Macromol. Rapid Commun.* **2012**, *33*, 287-295.
- (14) Tang, H. Y.; Zhang, D. H. *Polym. Chem.* **2011**, *2*, 1542-1551.
- (15) Saito, Y.; Lien, L. T. N.; Jinbo, Y. J.; Kumaki, J.; Narumi, A.; Kawaguchi, S. *Polym. J.* **2013**, *45*, 193-201.
- (16) Enomoto, H.; Nottelet, B.; Halifa, S. A.; Enjalbal, C.; Dupre, M.; Tailhades, J.; Coudane, J.; Subra, G.; Martinez, J.; Amblard, M. *Chem. Comm.* **2013**, *49*, 409-411.
- (17) Papadopoulos, P.; Floudas, G.; Klok, H. A.; Schnell, I.; Pakula, T. *Biomacromolecules* **2004**, *5*, 81-91.
- (18) Lu, H.; Cheng, J. J. *J. Am. Chem. Soc.* **2007**, *129*, 14114-14115.
- (19) Lu, H.; Cheng, J. J. *J. Am. Chem. Soc.* **2008**, *130*, 12562-12563.
- (20) Engler, A. C.; Shukla, A.; Puranam, S.; Buss, H. G.; Jreige, N.; Hammond, P. T. *Biomacromolecules* **2011**, *12*, 1666-1674.
- (21) Xiao, C.; Zhao, C.; He, P.; Tang, Z.; Chen, X.; Jing, X. *Macromol. Rapid Commun.* **2010**, *31*, 991-997.
- (22) Tang, H. Y.; Zhang, D. H. *Biomacromolecules* **2010**, *11*, 1585-1592.
- (23) Tang, H.; Li, Y.; Lahasky, S. H.; Sheiko, S. S.; Zhang, D. *Macromolecules* **2011**, *44*, 1491-1499.
- (24) Ding, J. X.; Xiao, C. S.; Zhao, L.; Cheng, Y. L.; Ma, L. L.; Tang, Z. H.; Zhuang, X. L.; Chen, X. S. *J. Polym. Sci., Part A: Polym. Chem.* **2011**, *49*, 2665-2676.
- (25) Ding, J.; Xiao, C.; Tang, Z.; Zhuang, X.; Chen, X. *Macromol. Biosci.* **2011**, *11*, 192-198.
- (26) Du, S.; Zhang, J.; Guan, Y.; Wan, X. *Aust. J. Chem.* **2014**, *67*, 39-48.
- (27) Zhou, S.; Zhou, Y.; Tian, H.; Zhu, Y.; Pan, Y.; Zhou, F.; Zhang, Q.; Shen, Z.; Fan, X. *J. Polym. Sci., Part A: Polym. Chem.* **2014**, 10.1002/pola.27167.
- (28) Zhou, Q. F.; Li, H. M.; Feng, X. D. *Macromolecules* **1987**, *20*, 233-234.
- (29) Chen, X.-F.; Shen, Z.; Wan, X.-H.; Fan, X.-H.; Chen, E.-Q.; Ma, Y.; Zhou, Q.-F. *Chem. Soc. Rev.* **2010**, *39*, 3072-3101.
- (30) Zhou, Q. F.; Zhu, X. L.; Wen, Z. Q. *Macromolecules* **1989**, *22*, 491-493.
- (31) Wan, X. H.; Zhang, F.; Wu, P. Q.; Zhang, D.; Feng, X. D.; Zhou, Q. F. *Macromol. Symp.* **1995**, *96*, 207-218.
- (32) Ma, Z.; Zheng, C.; Shen, Z.; Liang, D.; Fan, X. *J. Polym. Sci., Part A: Polym. Chem.* **2012**, *50*, 918-926.

- (33) Pan, Q. W.; Gao, L. C.; Chen, X. F.; Fan, X. H.; Zhou, Q. F. *Macromolecules* **2007**, *40*, 4887-4894.
- (34) Zhang, D.; Liu, Y. X.; Wan, X. H.; Zhou, Q. F. *Macromolecules* **1999**, *32*, 5183-5185.
- (35) Ye, C.; Zhang, H. L.; Huang, Y.; Chen, E. Q.; Lu, Y. L.; Shen, D. Y.; Wan, X. H.; Shen, Z. H.; Cheng, S. Z. D.; Zhou, Q. F. *Macromolecules* **2004**, *37*, 7188-7196.
- (36) Zhou, Q.-H.; Zheng, J.-K.; Shen, Z.; Fan, X.-H.; Chen, X.-F.; Zhou, Q.-F. *Macromolecules* **2010**, *43*, 5637-5646.
- (37) Zhang, B.; Groehn, F.; Pedersen, J. S.; Fischer, K.; Schmidt, M. *Macromolecules* **2006**, *39*, 8440-8450.
- (38) Kikuchi, M.; Lien, L. T. N.; Narumi, A.; Jinbo, Y.; Izumi, Y.; Nagai, K.; Kawaguchi, S. *Macromolecules* **2008**, *41*, 6564-6572.
- (39) Amitani, K.; Terao, K.; Nakamura, Y.; Norisuye, T. *Polym. J.* **2005**, *37*, 324-331.
- (40) Cheng, G.; Melnichenko, Y. B.; Wignall, G. D.; Hua, F.; Hong, K.; Mays, J. W. *Macromolecules* **2008**, *41*, 9831-9836.
- (41) Pesek, S. L.; Li, X.; Hammouda, B.; Hong, K.; Verduzco, R. *Macromolecules* **2013**, *46*, 6998-7005.
- (42) Gillissen, M. A. J.; Terashima, T.; Meijer, E. W.; Palmans, A. R. A.; Voets, I. K. *Macromolecules* **2013**, *46*, 4120-4125.
- (43) Sheiko, S. S.; Sun, F. C.; Randall, A.; Shirvanyants, D.; Rubinstein, M.; Lee, H.; Matyjaszewski, K. *Nature* **2006**, *440*, 191-194.
- (44) Guinier, A.; Fournet, A. *Small angle scattering of X-rays*; Wiley & Sons: New York, 1955.
- (45) Glatter, O.; Kratky, O. *Small Angle X-Ray Scattering*; Academic Press: London, 1982.
- (46) Konarev, P. V.; Volkov, V. V.; Sokolova, A. V.; Koch, M. H. J.; Svergun, D. I. *J. Appl. Crystallogr.* **2003**, *36*, 1277-1282.
- (47) Svergun, D. I. *J. Appl. Crystallogr.* **1992**, *25*, 495-503.
- (48) Rathgeber, S.; Pakula, T.; Wilk, A.; Matyjaszewski, K.; Lee, H.-i.; Beers, K. L. *Polymer* **2006**, *47*, 7318-7327.
- (49) Englebienne, P.; Hilbers, P. A. J.; Meijer, E. W.; De Greef, T. F. A.; Markvoort, A. J. *Soft Matter* **2012**, *8*, 7610-7616.
- (50) Temyanko, E.; Russo, P. S.; Ricks, H. *Macromolecules* **2001**, *34*, 582-586.
- (51) Fung, S. Y.; Keyes, C.; Duhamel, J.; Chen, P. *Biophys. J.* **2003**, *85*, 537-548.

TOC Graphic for

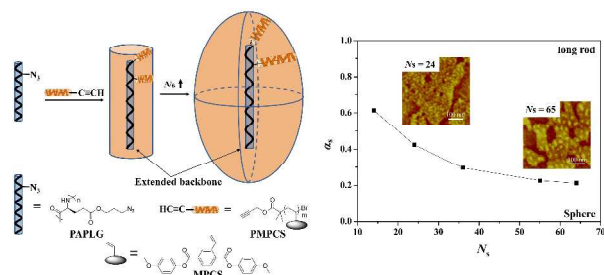
**Synthesis and Properties of a Rod-g-Rod Bottlebrush with a Semirigid Mesogen-Jacketed
Polymer as the Side Chain**

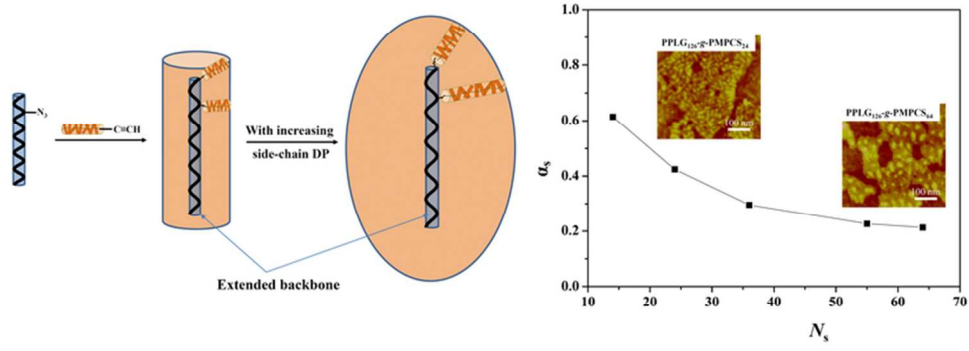
Hai-Jian Tian, Wei Qu, Yu-Feng Zhu, Zhihao Shen,* and Xing-He Fan*

Beijing National Laboratory for Molecular Sciences, Key Laboratory of Polymer Chemistry and
Physics of Ministry of Education, College of Chemistry and Molecular Engineering, Peking

University,

Beijing 100871, China





35x16mm (600 x 600 DPI)